Neuroscience Letters 501 (2011) 163–166

Contents lists available at ScienceDirect

Neuroscience Letters

journal homepage: www.elsevier.com/locate/neulet

Galectin-3 is upregulated in activated glia during Junin virus-induced murine encephalitis

Carolina Jaquenod De Giusti[a,1], Lucrecia Alberdi[a,1], Jesica Frik[a], María F. Ferrer[a], Emilia Scharrig[a], Mirta Schattner[b], Ricardo M. Gomez[a,*]

[a] Biotechnology and Molecular Biology Institute, CONICET-UNLP, La Plata, Argentina
[b] Thrombosis I Laboratory, Hematological Research Institute "Mariano R. Castex", National Academy of Medicine, CONICET, Buenos Aires, Argentina

ARTICLE INFO

Article history:
Received 3 June 2011
Received in revised form 2 July 2011
Accepted 5 July 2011

Keywords:
Astrocytes
Viral infection
GFAP
Microglia

ABSTRACT

Argentine haemorrhagic fever (AHF) is a systemic febrile syndrome characterized by several haematological and neurological alterations caused by Junín virus (JUNV), a member of the *Arenaviridae* family. Newborn mice are highly susceptible to JUNV and the course of infection has been associated with the viral strain used. Galectin-3 (Gal-3) is an animal lectin that has been proposed to play an important role in some central nervous system (CNS) diseases. In this study, we analysed Gal-3 expression at the transcriptional and translational expression levels during JUNV-induced CNS disease. We found that Candid 1 strain induced, with relatively low mortality, a subacute/chronic CNS disease with significant glia activation and upregulation of Gal-3 in microglia cells as well as in reactive astrocytes that correlated with viral levels. Our results suggest an important role for Gal-3 in viral-induced CNS disease.

Argentine haemorrhagic fever (AHF) is a systemic febrile syndrome that is characterised by several haematological alterations, and is caused by Junín virus (JUNV), a member of the *Arenaviridae* family [17]. Patients with AHF frequently present with central nervous system (CNS) involvement in the acute period [15]. In addition, although treatment with serum from convalescent patients reduces mortality from 30% to 1%, about 10–15% of patients who receive this treatment present with delayed neurological syndrome [7]. Interestingly, pathological findings in the CNS of both humans and animal models do not reflect the severity of the disease [3,4]. In addition, although it has been shown in animals that JUNV can reach the CNS via a neural route [13], the mechanism(s) behind JUNV pathogenesis remain poorly understood. Newborn mice are extremely susceptible to JUNV, and high lethality (>90%) has been reported upon exposure to virulent strains [4]. Histopathological studies found that relatively mild meningo-encephalitis correlated with JUNV antigen detection in the cytoplasm of neurons, and to a lesser extent, in the cytoplasm of astrocytes; however, neurons do not usually show major alterations [6,11]. In surviving animals, the chronic stage of AHF is characterised by a gradual disappearance of JUNV antigen, coupled with glial activation (including a prominent astrocyte reaction associated with enhanced glial fibrillary acid protein (GFAP) expression) and a lack of correlation with the distribution of viral antigens [12].

Galectins are members of a growing family of β-galactoside-binding animal lectins, composed of one or two carbohydrate-recognition domains (CRDs), containing approximately 130 amino acids each [14,22]. Galectin-3 (Gal-3) has been shown to play a pivotal role in diverse physiological functions, such as cell growth, apoptosis, and mRNA splicing; as well as in pathological processes, as an inflammatory mediator [26]. Although Gal-3 has also been associated with microglial activation in mouse brains in a mouse model of experimental autoimmune disease [23], its role in the CNS under pathological conditions is poorly understood.

C57BL/6 mice were obtained from the Veterinary School, UNLP. JUNV vaccine Candid 1 strain (C#1) and viral stock preparations were described previously [5,16]. Groups of 12 newborn (<48 h old) animals were inoculated, intracerebrally (ic) with 20 μL of virus, containing 10^2 or 10^4 plaque-forming units (PFU). Control mice received an equal volume of mock-infected Vero cell supernatants. All animals received water and food *ad libitum*.

Mice were sacrificed (with the exception of spontaneous death) at 10 (acute) or 40 (subacute/chronic) days post-inoculation (dpi), and their brains were harvested. One hemisphere was frozen at −70 °C for later RNA or protein extraction, and the other was fixed with 4% buffered paraformaldehyde, for subsequent histological examination and immunohistochemical staining.

Paraffin-embedded, 6-μm thick sections from fixed brain samples were stained with haematoxylin and eosin (H&E). Rat

* Corresponding author at: Instituto de Biotecnología y Biología Molecular, Facultad de Ciencias Exactas, Universidad Nacional de La Plata, Calle 49 y 115, 1900 La Plata, Argentina. Tel.: +54 0221 422 6977; fax: +54 0221 422 4967.
E-mail address: rmg@biol.unlp.edu.ar (R.M. Gomez).
[1] Equally contributing authors.

0304-3940/$ – see front matter © 2011 Elsevier Ireland Ltd. All rights reserved.
doi:10.1016/j.neulet.2011.07.007

monoclonal anti-Gal-3 (M3/38 hybridoma) antibodies were used for Gal-3 detection. Rabbit polyclonal anti-F4/80 (Abcam, USA) and anti-GFAP (Dako, Denmark) antibodies were used to detect activated microglia and astrocytes, respectively [2]. Anti-species biotinylated antibodies and peroxidase-conjugated streptavidin were purchased from Dako (Denmark). FITC-conjugated anti-rabbit antibodies and Alexa 546-conjugated goat anti-rat antibodies were purchased from Invitrogen (USA). Immunoperoxidase labelling and immunofluorescence staining was performed as previously described [6,20].

Total RNA samples from mouse brains were extracted using TriReagent (Molecular Research Center), according to the manufacturer's instructions. cDNA was synthesised from 1 μg of total RNA by reverse transcription using MMLV reverse transcriptase (Promega, Argentina) and random hexamers (Byodinamics, Argentina). After incubation for 1 h at 42 °C, samples were heat-inactivated and kept at 4 °C until further use. One μL of cDNA from each sample was used for Real-Time PCR (qPCR), as described previously [21], with minor differences. Briefly, PCR amplification and analysis was performed with a Line-Gene instrument (Bioer) and LineGene K Flourescence Quantitative Detection System (Version 4.0.00 software). The TAQurate™ GREEN Real-Time PCR MasterMix (Epicentre) was used for all reactions, following the manufacturer's instructions. Normalised expression values were calculated from absolute quantities of the gene of interest and a housekeeping gene. Standard curves for absolute quantification were generated from purified amplicons, following confirmation of their sequences. The concentrations of standard stocks, expressed as the number of amplicon copies per volume unit, were calculated from their absorbance at 260 nm. Stock solutions were serially diluted 10-fold, to obtain a standard series ranging from 10^7 to 10^4 copies of amplicon per μL of standard. The primers used were as follow: β-actin F 5′CGTCATCCATGGCGAACTG3′; β-actin R 5′GCTTCTTTGCAGCTCCTTCGT 3′; GFAP F 5′TCCTGGAACAGCAAAACAAG3′; GFAP R 5′CAGCCTCAGGTTGGTTTCAT3′; Gal-3 F: 5′GACCACTGACGGTGCCCTAT3′; Gal-3 R: 5′GGGGTTAAAGTGGAAGGCAA3′; JUNV F 5′CGCACAGTAAGGGGATCCTAGGC3′; JUNV R 5′GGCATCCTTCAGAACATC3′; and ionised calcium-binding adapter molecule 1 (Iba1) F 5′CAGACTGCCAGCCTAAGACA3′; Iba1 R 5′ AGGAATTGCTTGTTGATCCC3′ as marker of activated microglia [2].

Total brain lysates from mock and JUNV-infected mice were obtained by homogenisation in RIPA buffer [5]. Western blotting was performed as previously described [5]. Briefly, protein samples were separated by SDS-PAGE on 10% polyacrylamide gels and transferred to PVDF membranes. Blotted membranes were incubated overnight at 4 °C with PBS 0.1% Tween-20 (PBST) 5% skimmed milk. After washing with PBST, membranes were incubated with one of the following primary antibodies: mouse monoclonal anti-β-actin (GenScript), or the already described anti-Gal-3, anti-GFAP, anti-F4/80 (Abcam) or our own rabbit polyclonal anti-N protein of JUNV for 1 h at 37 °C. Membranes were washed again and incubated with anti-mouse-HRP (Santa Cruz Biotechnology), anti-rat biotinylated (Dako), or anti-rabbit HRP (Dako) secondary antibodies, respectively, for another hour at 37 °C. Membranes incubated with anti-rat biotinylated antibody were incubated for a further hour at 37 °C with streptavidin HRP (Dako). Bands were detected by enhanced chemiluminescence (ECL) (Amersham) and quantified using LabWorksTM 4.6 (Image Acquisition and Analysis Software).

All newborn animals inoculated with 10^4 PFU of the C#1 strain of JUNV died before 21 dpi; while, in contrast, those receiving 10^2 PFU had a 30% mortality rate at the end of the observation period (spontaneous death was not observed in mock-infected animals). Viral infection was confirmed by qPCR in all JUNV-infected animals, and no virus was detected in mock-infected animals (data not shown).

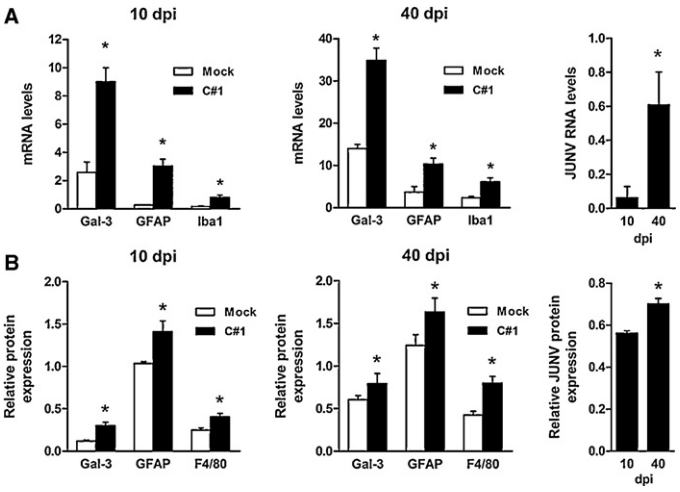

Fig. 1. Upregulation of Gal-3 in JUNV-infected mice correlated with glia activation markers. (A) Real-time PCR shows enhanced transcription of Gal-3, GFAP and Iba1, in samples taken from the brains of animals inoculated with C#1 versus mock-infected animals, at 10 and 40 dpi. (B) Western blot analysis: Gal-3, GFAP and F4/80 protein expression at 10 and 40 dpi were also higher in the brains of animals inoculated with C#1 versus mock-infected animals. Both RNA (A) and protein levels (B) of JUNV were higher at 40 dpi compared to 10 dpi. Results are representative of three different experiments. *, $p < 0.05$.

Significantly higher levels of both JUNV RNA and protein were detected at 40 dpi versus 10 dpi (Fig. 1A and B). After normalisation with actin (a housekeeping gene), qPCR revealed significantly higher levels of Gal-3 mRNA, GFAP, and Iba1, in samples collected at both 10 and 40 dpi versus uninfected controls (Fig. 1A). In general, Western blotting analysis supports these qPCR results (see Fig. 1B) with both procedures showing higher levels at 40 dpi compared to 10 dpi.

Based on H&E staining, mock-infected mice showed no signs of disease in the acute (Fig. 2A) or chronic stage (data not shown). In contrast, C#1-infected animals showed signs of mild meningoencephalitis, such as brain congestion, perivascular cuffing of polymorphs and mononuclear cells, little neuronal necrosis, and moderate cerebral infiltration of inflammatory cells during the acute stage (Fig. 2B); which persisted until the end of the observation period (data not shown).

In order to examine the tissue distribution of Gal-3, GFAP and F4/80 antigens, sections from control and JUNV-infected mouse brains were analysed by immunohistochemistry. At 10 dpi, Gal-3, GFAP and F4/80 immunoreactivity was almost undetectable in the brains of mock-infected mice, and only slightly visible in the CNS of JUNV-infected mice (data not shown). At 40 dpi, control samples showed clear GFAP staining (Fig. 3E and F), but very

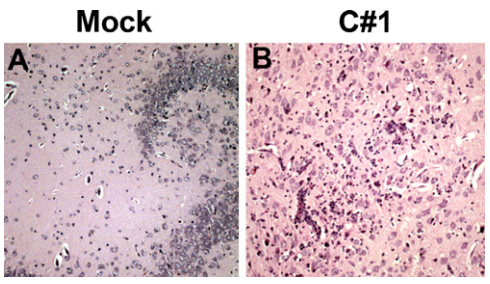

Fig. 2. Histopathology of JUNV-infected animals. Representative haematoxylin and eosin staining of hippocampus sections from mock- (A) or C#1-infected animals (B). Control animals showed normal tissue; whereas C#1-infected animals at 10 dpi showed moderate parenchymal infiltration of mononuclear cells, some neuronal necrosis, and small vessels with perivascular cuffing. Similar observations were made at 40 dpi. 200×.

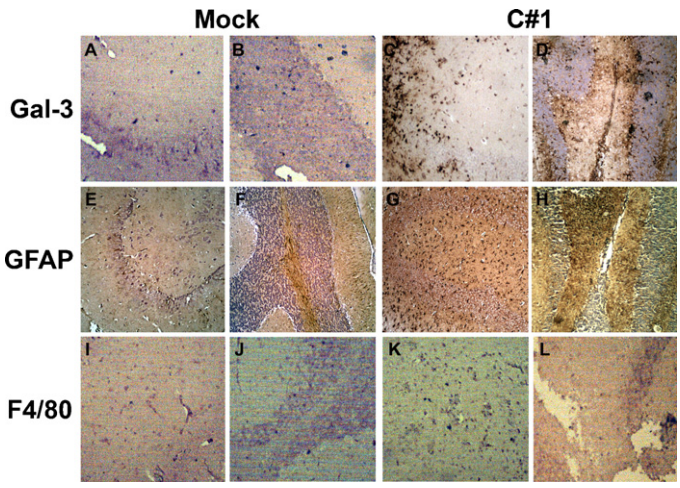

Fig. 3. Tissue distribution of Gal-3, GFAP and Iba1 in JUNV-infected animals. Representative slides from immunohistochemical staining of Gal-3, GFAP and F4/80, on hippocampus and cerebellum sections of mock-infected mice (A–B, E–F and I–J), and C#1-infected mice at 40 dpi (C-D, G-H and K-L), respectively, showing different antigen distribution patterns. Slides were counterstained with haematoxylin. 150×.

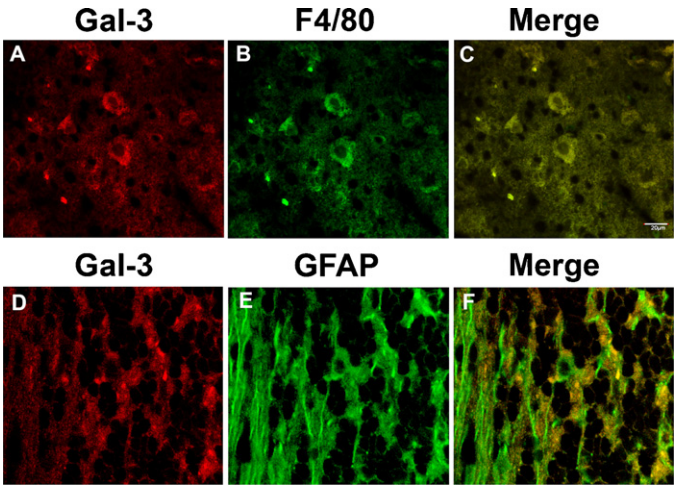

Fig. 4. Confocal microscopy analysis of Gal-3, F4/80 or GFAP JUNV-infected animals at 40 dpi. Confocal image following double-immunostaining for Gal-3 and F4/80. Most Gal3-positive cells (A) were also positive for F4/80 (B). The merged image is shown in (C). In addition, some Gal-3-positive cells (D) were also GFAP-positive (E). The merged image is shown in (F). Scale bar, 20 μm.

faint Gal-3 and F4/80 immunolabelling (Fig. 3 A–B and I–J, respectively). In contrast, in C#1-infected samples, an increased number of immunoreactive Gal-3, GFAP and F4/80 cells was observed (Fig. 3 C–D, G–H and K–L, respectively).

In addition, most F4/80-positive cells were found in close proximity to other mononuclear cells suggesting the presence of an infiltrating cell exudate. In contrast, activated astrocytes (GFAP-positive cells) showed a more lesion-independent distribution. For Gal-3-positive cells, immunohistochemistry results suggest the presence of both infiltrating macrophages and activated microglia, and, in some cases, activated astrocytes.

Finally, to identify cells expressing Gal-3, CNS sections from JUNV-infected mice were double-labelled and analysed by confocal immunofluorescence microscopy: revealing that most of the F4/80 positive cells and some GFAP positive cells were also positive for Gal-3 (Fig. 4A–F).

Although the capacity of several JUNV strains to induce experimental murine CNS disease has been extensively investigated [4]; the C#1 strain has only been examined in terms of mortality rates versus age [18]. Therefore, in the present study, we further characterised this experimental model in order to enable investigations into the disease at the subacute/chronic stage. In fact, while infecting mice with 10^4 PFU resulted in 100% mortality, a 100-fold decrease in viral inoculum still induced CNS disease in all inoculated animals, with a relatively low mortality (30%).

To the best of our knowledge, this is the first description of an experimental model of C#1-induced CNS disease.

To study the expression of Gal-3 in this system, we correlated Gal-3 levels with JUNV burden, at both the transcriptional and translational levels, coupled with the degree of glial activation. Interestingly, we found an increase in glial activation with time, which correlated with significantly higher levels of Gal-3 and JUNV at both the RNA and protein levels.

Immunohistochemistry analysis clearly demonstrates an increase in Gal-3, GFAP and F4/80 positive cells at 40 dpi, although the tissue distribution was not similar. Double-labelling analysis revealed that most Gal-3-positive cells were activated microglia; whereas some cells with an astrocyte phenotype also showed colocalisation of Gal-3 and GFAP, in agreement with recent studies on hypoxia–ischemia [2,27]. However, these observations are in contrast with previous studies conducted on a mouse model of prion disease, where Gal-3 was expressed only in brain macrophages/microglia, but not in activated astrocytes [9]. Although this apparent contradiction may be explained by differences between these diseases; it should be noted that because Gal-3 expression is lower in astrocytes than activated microglia, astrocytes may require a certain degree of activation before Gal-3 can be detected by this technique. In any case, the ability of astrocytes to express Gal-3 has been confirmed in recent *in vitro* studies [8].

The functional roles of Gal-3 in the CNS have only recently begun to emerge [1,8,23]. Considering that Gal-3 induces the activation of chemokine receptors [25], and is a potent chemoattractant molecule for monocytes and macrophages associated with the phagocytosis of microorganisms and apoptotic cells [24], it is conceivable that increased expression of Gal-3 in JUNV-induced CNS disease might be involved in the phagocytosis of infected cells.

Both detrimental and beneficial roles have been associated with enhanced Gal-3 expression in the CNS. For example, in an experimental prion disease model, increased Gal-3 expression has been associated with a detrimental role in activated microglia [19]. On the other hand, in cerebral ischemia, it has been suggested that some Gal-3-positive cells represent a specific population of insulin-like growth factor I-positive resident microglial cells, with protective rather than damaging properties [10]. Because astrocyte activation may represent a beneficial cell response to viral-induced CNS damage [6], the role of Gal-3 expression in reactive astrocytes in viral-induced CNS damage must be determined.

In conclusion, we report the first description of a murine CNS disease induced by the C#1 strain of JUNV. The use of the C#1 strain is advantageous for biosafety reasons, and because of its wide availability. Since JUNV-induced CNS disease is strain dependent, the use of the C#1 strain in future studies may enable more standardised comparisons. We also present the first study of Gal-3 expression in a viral-induced CNS disease, and propose that Gal-3 expression by activated microglia/macrophages and astrocytes after viral CNS infection may play a role in the subsequent CNS disease. Further experiments using a transgenic animal model, such as Gal-3 knockout mice, may help us better understand the specific role of Gal-3 in the pathogenesis of JUNV-induced CNS disease.

Acknowledgments

This work was supported by the Universidad Nacional de La Plata (Project X592) and ANPCyT (PICT 07-00028 and 07-00642). MS and RMG are researchers and CJG is a fellow of the Consejo Nacional de Investigaciones Científicas y Técnicas (CONICET), Argentina.

References

[1] C.M. Alves, D.A. Silva, A.E. Azzolini, C.M. Marzocchi-Machado, J.V. Carvalho, A.C. Pajuaba, Y.M. Lucisano-Valim, R. Chammas, F.T. Liu, M.C. Roque-Barreira, J.R. Mineo, Galectin-3 plays a modulatory role in the life span and activation of murine neutrophils during early Toxoplasma gondii infection , Immunobiology 215 (2010) 475–485.
[2] C. Doverhag, M. Hedtjarn, F. Poirier, C. Mallard, H. Hagberg, A. Karlsson, K. Savman, Galectin-3 contributes to neonatal hypoxic-ischemic brain injury , Neurobiol. Dis. 38 (2010) 36–46.
[3] B. Elsner, E. Schwarz, O.G. Mando, J. Maiztegui, A. Vilches, Pathology of 12 fatal cases of Argentine hemorrhagic fever , Am. J. Trop. Med. Hyg. 22 (1973) 229–236.
[4] R.M. Gomez, C. Jaquenod de Giusti, M.M. Sanchez Valduvi, J. Frik, M.F. Ferrer, M. Schattner, Junin virus. A XXI century update , Microbes Infect. 13 (2011) 303–311.
[5] R.M. Gomez, R.G. Pozner, M.A. Lazzari, L.P. D'Atri, S. Negrotto, A.M. Chudzinski-Tavassi, M.I. Berria, M. Schattner, Endothelial cell function alteration after Junin virus infection , Thromb. Haemost. 90 (2003) 326–333.
[6] R.M. Gomez, A. Yep, M. Schattner, M.I. Berria, Junin virus-induced astrocytosis is impaired by iNOS inhibition , J. Med. Virol. 69 (2003) 145–149.
[7] L.H. Harrison, N.A. Halsey, K.T. McKee Jr., C.J. Peters, J.G. Barrera Oro, A.M. Briggiler, M.R. Feuillade, J.I. Maiztegui, Clinical case definitions for Argentine hemorrhagic fever , Clin. Infect. Dis. 28 (1999) 1091–1094.
[8] S.B. Jeon, H.J. Yoon, C.Y. Chang, H.S. Koh, S.H. Jeon, E.J. Park, Galectin-3 exerts cytokine-like regulatory actions through the JAK-STAT pathway , J. Immunol. 185 (2010) 7037–7046.
[9] J.K. Jin, Y.J. Na, J.H. Song, H.G. Joo, S. Kim, J.I. Kim, E.K. Choi, R.I. Carp, Y.S. Kim, T. Shin, Galectin-3 expression is correlated with abnormal prion protein accumulation in murine scrapie , Neurosci. Lett. 420 (2007) 138–143.
[10] M. Lalancette-Hebert, G. Gowing, A. Simard, Y.C. Weng, J. Kriz, Selective ablation of proliferating microglial cells exacerbates ischemic injury in the brain , J. Neurosci. 27 (2007) 2596–2605.
[11] E.F. Lascano, M.I. Berria, Immunoperoxidase study of astrocytic reaction in Junin virus encephalomyelitis of mice , Acta. Neuropathol. (Berl.) 59 (1983) 183–190.
[12] E.F. Lascano, M.I. Berria, M.M. Avila, M.C. Weissenbacher, Astrocytic reaction predominance in chronic encephalitis of Junin virus-infected rats , J. Med. Virol. 29 (1989) 327–333.
[13] E.F. Lascano, G.D. Lerman, J.L. Blejer, R.L. Caccuri, M.I. Berria, Immunoperoxidase tracing of Junin virus neural route after footpad inoculation , Arch. Virol. 122 (1992) 13–22.
[14] F.T. Liu, R.J. Patterson, J.L. Wang, Intracellular functions of galectins , Biochim. Biophys. Acta 1572 (2002) 263–273.
[15] J.I. Maiztegui, Clinical and Epidemiological Patterns of Argentine Haemorrhagic Fever , Bull. WHO, 1975, pp. 385–575.
[16] J.I. Maiztegui, K.T. McKee Jr., J.G. Barrera Oro, L.H. Harrison, P.H. Gibbs, M.R. Feuillade, D.A. Enria, A.M. Briggiler, S.C. Levis, A.M. Ambrosio, N.A. Halsey, C.J. Peters, Protective efficacy of a live attenuated vaccine against Argentine hemorrhagic fever. AHF Study Group , J. Infect. Dis. 177 (1998) 277–283.
[17] R.F. Marta, V.S. Montero, F.C. Molinas, Systemic disorders in Argentine haemorrhagic fever , Bull. Inst. Pasteur. 96 (1998) 115–124.
[18] S.I. Medeot, M.S. Contigiani, E.R. Brandan, M.S. Sabattini, Neurovirulence of wild and laboratory Junin virus strains in animal hosts , J. Med. Virol. 32 (1990) 171–182.
[19] S.W. Mok, C. Riemer, K. Madela, D.K. Hsu, F.T. Liu, S. Gultner, I. Heise, M. Baier, Role of galectin-3 in prion infections of the CNS , Biochem. Biophys. Res. Commun. 359 (2007) 672–678.
[20] R.G. Pozner, S. Collado, C.J. de Giusti, A.E. Ure, M.E. Biedma, V. Romanowski, M. Schattner, R.M. Gomez, Astrocyte response to Junin virus infection , Neurosci. Lett. 445 (2008) 31–35.
[21] G. Prêtre, N. Olivera, M. Cédola, S. Haase, L. Alberdi, B. Brihuega, R.M. Gómez, Role of inducible nitric oxide synthase in the pathogenesis of experimental leptospirosis , Microb. Pathog. 51 (2011) 203–208.
[22] G.A. Rabinovich, M.A. Toscano, S.S. Jackson, G.R. Vasta, Functions of cell surface galectin–glycoprotein lattices , Curr. Opin. Struct. Biol. 17 (2007) 513–520.
[23] F. Reichert, S. Rotshenker, Galectin-3/MAC-2 in experimental allergic encephalomyelitis , Exp. Neurol. 160 (1999) 508–514.
[24] H. Sano, D.K. Hsu, J.R. Apgar, L. Yu, B.B. Sharma, I. Kuwabara, S. Izui, F.T. Liu, Critical role of galectin-3 in phagocytosis by macrophages , J. Clin. Invest. 112 (2003) 389–397.
[25] H. Sano, D.K. Hsu, L. Yu, J.R. Apgar, I. Kuwabara, T. Yamanaka, M. Hirashima, F.T. Liu, Human galectin-3 is a novel chemoattractant for monocytes and macrophages , J. Immunol. 165 (2000) 2156–2164.
[26] V. Sundblad, D.O. Croci, G.A. Rabinovich, Regulated expression of galectin-3, a multifunctional glycan-binding protein, in haematopoietic and non-haematopoietic tissues , Histol. Histopathol. 26 (2011) 247–265.
[27] Y.P. Yan, B.T. Lang, R. Vemuganti, R.J. Dempsey, Galectin-3 mediates post-ischemic tissue remodeling , Brain Res. 1288 (2009) 116–124.